

# Modeling Thermally Activated Delayed Fluorescence

Master's thesis  
University of Turku  
Theoretical Physics  
2025  
Israt Jahan Suhi  
Examiners:  
Docent Kimmo Luoma  
Dr. Olli Siltanen

The originality of this thesis has been checked in accordance with the University of Turku quality assurance system using Turnitin Originality Check service.

UNIVERSITY OF TURKU  
Department of Physics and Astronomy

**Israt Jahan Suhi** Modeling Thermally Activated Delayed Fluorescence

Pro Gradu, 55 p.  
Theoretical Physics  
December 2025

---

Thermally activated delayed fluorescence (TADF) has emerged as a key mechanism to enhance the efficiency of organic light-emitting devices by harvesting both singlet and triplet excitons. In this thesis, we present a detailed theoretical study of TADF using multi-level rate equation models, starting from the basic three-level system and extending to general multi-level singlet ( $S_m$ ) and triplet ( $T_n$ ) configurations. Analytical solutions for population dynamics are derived, revealing how excitons redistribute among higher singlet and triplet states over time. The results clearly show the origin of delayed fluorescence and provide insight into the interplay of radiative and non-radiative channels. This work presents a theoretical framework for predicting and optimizing TADF behavior in novel organic materials.

Keywords: Thermally activated delayed fluorescence, intersystem crossing, Reverse intersystem crossing, singlet-triplet energy gap, radiative and non-radiative decay, kinetic modeling, analytical rate-equation model.

## Acknowledgments

I would like to express my sincere gratitude to my supervisor, Kimmo Luoma, and co-supervisor, Olli Siltanen, for their guidance, support, and valuable feedback throughout the course of this work. Their expertise and guidance were essential to the completion of this thesis.

I am also grateful to the University of Turku for providing a stimulating academic environment and the necessary resources to carry out this research.

Finally, I am deeply thankful to my spouse for his constant support, patience, and understanding throughout my studies.

# Contents

<b>1</b>	<b>Introduction</b>	<b>1</b>
<b>2</b>	<b>Literature Overview</b>	<b>3</b>
2.1	Introduction to Organic Electroluminescence and Motivation for TADF Modeling . . . . .	3
2.2	Historical Development and Significance of TADF . . . . .	4
2.3	Photophysical Foundations of TADF . . . . .	5
2.4	Exciton Dynamics and Kinetic Representations . . . . .	7
2.5	Thermodynamic and Quantum-Mechanical Basis of TADF . . . . .	8
2.6	Molecular Factors Influencing Analytical Parameters . . . . .	10
2.7	Analytical Treatments of RISC: Marcus and Marcus–Levich–Jortner Frameworks . . . . .	11
2.8	Density-Matrix and Master-Equation Approaches . . . . .	12
2.9	Analytical Expressions for Quantum Yield and Efficiency . . . . .	13
2.10	Limitations and Open Problems in Analytical Descriptions . . . . .	15
2.11	Summary of the Literature Review . . . . .	16
<b>3</b>	<b>Relevant Models</b>	<b>16</b>
3.1	Kinetic Rate Equation Models . . . . .	17
3.2	Analytical Expressions for Quantum Yields and Lifetimes . . . . .	20
3.3	Temperature Dependence and Arrhenius Analysis . . . . .	21
3.4	Spin Statistical and Exciton-Formation Models . . . . .	23
3.5	Marcus and Marcus-Levich-Jortner (MLJ) Analytical Treatments . . . . .	25
3.6	Density Matrix and Quantum Master Equation Approaches . . . . .	26
3.7	Analytical Modeling of Device Efficiency . . . . .	28
3.8	Extended Analytical Models . . . . .	30
3.9	Summary . . . . .	31

<b>4</b>	<b>Generic Model and Results</b>	<b>32</b>
4.1	Three-State Kinetic Model . . . . .	33
4.2	Extension to Higher Excited States . . . . .	41
4.3	Results . . . . .	46
<b>5</b>	<b>Conclusion</b>	<b>51</b>

# 1 Introduction

Organic light-emitting diodes (OLEDs) are widely used in modern display and light technologies because of their low power consumption, flexibility, and the wide range of colors they can produce. Even with these advantages, improving their efficiency is still an important challenge. In conventional fluorescent OLEDs, this problem is closely linked to spin statistics: when electrons and holes recombine, only about 25% of the resulting excitons are in singlet states that can emit light directly, while the remaining 75% form triplet states that are usually non-emissive. Finding ways to make use of these triplet excitons have therefore been a central goal in OLED research.

Thermally activated delayed fluorescence (TADF) offers a way to address this limitation. In TADF materials, triplet excitons can be converted back into singlet excitons through reverse intersystem crossing (RISC), provided that the energy gap between the singlet and triplet states is small enough. Thermal energy then allows this upconversion process to occur, enabling triplets to contribute to light emission. This makes it possible, at least in principle, to achieve nearly 100% internal quantum efficiency using mostly organic materials, without relying too much on heavy metals as in phosphorescent OLEDs. Although for RISC, some heavy element is still needed to have spin-orbit coupling.

From a theoretical point of view, TADF involves several coupled processes taking place between different excited states. These include radiative and non-radiative decay, intersystem crossing, reverse intersystem crossing, and interaction between multiple singlet and triplet levels. Over the years, many models have been proposed to describe these dynamics, often using systems of rate equations. Simple models are useful for building intuition, but they can miss important features seen in experiments, such as temperature-dependent emission, long delayed fluorescence lifetimes, or the influence of higher-lying excited states.

The main goal of this thesis is to build analytical model for TADF that remain physically transparent while still capturing the key dynamical features of the system. The thesis begins with a literature review that introduces the basic physical mechanisms behind TADF and summarizes the most common modeling approaches used in the field. This is followed by a discussion of other related models that describe excited-state dynamics in organic materials and that help motivate the assumptions made later on.

The central part of the thesis focuses on the three-level model of TADF, consisting of the ground state, a lowest excited singlet state, and a triplet state. Despite its simplicity, this model already captures the essential physics behind delayed fluorescence. The corresponding rate equations are derived and solved analytically, leading to explicit expressions for the time evolution of the state populations and the resulting emission. These results make it easier to see how different physical parameters affect TADF behavior.

The model is then extended to include multiple singlet and triplet excited states, which is closer to the situation in real TADF materials. In this extended framework, a general analytical solution is developed, allowing the role of higher-lying states to be studied in a systematic way. The simpler three-level model emerges as a special case of this more general treatment, providing a clear link between the different levels of description.

Overall, this thesis aims to present a clear and step-by-step analytical treatment of TADF based on rate-equation models. By moving gradually from simple to more general systems, the work highlights the physical mechanisms that control delayed fluorescence and provides a solid foundation for further theoretical or experimental studies of TADF-based OLEDs.

## 2 Literature Overview

### 2.1 Introduction to Organic Electroluminescence and Motivation for TADF Modeling

Organic electroluminescence (EL) is the process by which organic semiconductors emit light when an electric current passes through them, rather than when they are illuminated by another light source. Since Tang and Van-Slyke demonstrated the first multilayer organic light-emitting diode (OLED) in 1987[1], these devices have become key components of modern display and lighting technologies. Their popularity comes from several advantages—they are flexible, thin, lightweight, and allow easy control of color. The basic idea is simple: injected electrons and holes meet inside the organic layer, form excitons, and these excitons either emit light or lose their energy without emitting it[2].

A central concept in organic light emission is spin statistics. When electrons and holes recombine, they form roughly 25% singlet excitons and 75% triplet excitons. In normal fluorescent materials, only singlets can emit light efficiently because triplet emission is spin-forbidden in organic molecules with weak spin-orbit coupling (SOC). As a result, fluorescent OLEDs can reach only up to 25% internal quantum efficiency (IQE)[3]. To overcome this, heavy-metal complexes such as Ir(III) and Pt(II) were later introduced to enhance SOC and enable triplet emission[4]. However, these materials are costly, less tunable in color, and tend to degrade more quickly during operation.

Thermally activated delayed fluorescence (TADF) provides a fully organic and much more versatile way to harvest triplet excitons[5]. In TADF molecules, the energy gap between the lowest singlet and triplet states ( $\Delta E_{ST}$ ) is made very small. This allows triplet excitons to be thermally converted back into singlets through a process called *reverse intersystem crossing* (RISC). By recycling triplets in this

way, nearly all excitons can contribute to light emission, allowing OLEDs to reach efficiencies close to 100%. Because RISC depends strongly on temperature and energy levels, being able to model and predict these transition rates is crucial for designing efficient TADF molecules. Therefore, developing analytical models that link molecular structure, energy levels, and rate constants has become a central research focus in the study of TADF.

## 2.2 Historical Development and Significance of TADF

The concept of delayed fluorescence has been known for a long time. It was first observed in the 1960s in anthracene-based compounds, but at that time it was mainly considered a scientific curiosity rather than a practical method for generating light. For several decades, this phenomenon remained unexplored in the context of light-emitting devices. It was not until the early 2010s that researchers recognized its potential for achieving highly efficient organic light-emitting diodes (OLEDs).

A major turning point came in 2012, when Adachi and co-workers reported the molecule 4CzIPN (2,4,5,6-tetrakis(carbazol-9-yl)isophthalonitrile)[5]. Their groundbreaking work showed that a purely organic emitter could achieve nearly 100% internal quantum efficiency (IQE) by exploiting the principle of thermally activated delayed fluorescence (TADF). This discovery demonstrated that both singlet and triplet excitons could be harvested efficiently without relying on heavy-metal atoms. It marked the beginning of what is now referred to as the third generation of OLED emitters—following the first generation of fluorescent emitters and the second generation of phosphorescent ones[4].

Following this discovery, research into TADF emitters expanded rapidly. Scientists developed a wide variety of molecules capable of emitting light across nearly the entire visible spectrum. Green and orange TADF emitters soon achieved external quantum efficiencies (EQEs) above 20%, while blue TADF OLEDs later surpassed

30% EQE[6]. These advances established TADF as a promising approach for creating energy-efficient, color-tunable, and environmentally friendly OLED technologies.

Beyond display and lighting applications, TADF materials have also found use in other areas such as photo-catalysis, sensing, and bio-imaging[7]. Their ability to manage triplet states without heavy metals makes them attractive for systems that require precise control over excited-state dynamics and efficient light–matter interactions.

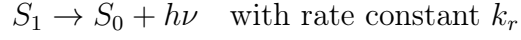
Despite these remarkable achievements, the microscopic details that govern TADF are still not fully understood. In particular, the relationships between energetic parameters (such as the singlet–triplet energy gap,  $\Delta E_{ST}$ ) and kinetic parameters (such as the rates of intersystem crossing and reverse intersystem crossing) remain areas of active research. In many cases, device optimization has relied heavily on empirical trial and error rather than on predictive theoretical or analytical models[8].

This gap highlights the importance of developing robust analytical frameworks that can directly connect experimentally measurable properties—such as delayed fluorescence lifetimes and quantum yields—to microscopic molecular parameters like  $\Delta E_{ST}$ , spin–orbit coupling strength, reorganization energy, and rate constants. Building and refining these analytical models is essential for interpreting experiments and guiding the rational design of next-generation TADF materials. This analytical perspective forms one of the main motivations of this thesis.

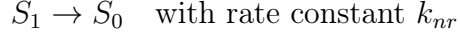
### 2.3 Photophysical Foundations of TADF

At the microscopic level, thermally activated delayed fluorescence (TADF) involves the interaction among four main electronic states: the ground singlet state ( $S_0$ ), the first excited singlet state ( $S_1$ ), and the lowest triplet levels ( $T_1$ , and sometimes higher triplets such as  $T_n$ ). The main photophysical processes connecting these states can be summarized as follows:

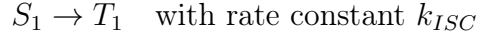
- **Radiative decay (fluorescence):**



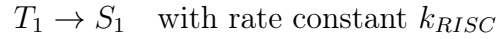
- **Non-radiative decay:**



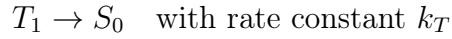
- **Intersystem crossing (ISC):**



- **Reverse intersystem crossing (RISC):**



- **Triplet decay (phosphorescence or quenching):**



The time evolution of the singlet and triplet populations can be described by a set of coupled rate equations:

$$\frac{dN_S}{dt} = G_S - (k_r + k_{nr} + k_{ISC})N_S + k_{RISC}N_T, \quad (2.1)$$

$$\frac{dN_T}{dt} = G_T + k_{ISC}N_S - (k_T + k_{RISC})N_T, \quad (2.2)$$

where  $N_S$  and  $N_T$  represent the populations of the  $S_1$  and  $T_1$  states, respectively, and  $G_S$ ,  $G_T$  are the generation rates of singlet and triplet excitons under optical or electrical excitation[2]. Solving these equations under steady-state or time-resolved conditions forms the basis of most analytical treatments of TADF kinetics.

A crucial condition for efficient TADF is a small singlet–triplet energy gap:

$$\Delta E_{ST} = E(S_1) - E(T_1) \lesssim 0.2\text{eV}.$$

This ensures that the available thermal energy at room temperature ( $k_B T \approx 0.026\text{eV}$  at 300 K) can drive the reverse intersystem crossing process according to an Arrhenius-type relationship:

$$k_{RISC} = A_{RISC} \exp\left(-\frac{\Delta E_{ST}}{k_B T}\right),$$

where  $A_{RISC}$  accounts for the spin-orbit coupling (SOC) and vibronic coupling contributions.

In practice, molecular design strategies aim to minimize  $\Delta E_{ST}$  while enhancing SOC and vibronic interactions to increase the RISC rate[9]. Experimentally, TADF emission typically shows two components: a prompt fluorescence on the nanosecond scale and a delayed fluorescence on the microsecond-to-millisecond scale. The delayed portion becomes stronger as temperature rises, confirming the thermally activated nature of RISC[10]. Analyzing this biexponential decay behavior allows researchers to extract rate constants and better understand molecular performance in TADF systems.

## 2.4 Exciton Dynamics and Kinetic Representations

Exciton dynamics describe how singlet and triplet populations evolve after excitation. In the weak excitation regime, where exciton-exciton interactions are negligible, the basic kinetic model is usually sufficient. Solving the rate equations leads to biexponential decay of the total emission intensity,

$$I(t) = k_r N_S(t),$$

which can be written as

$$I(t) = A_p e^{-t/\tau_p} + A_d e^{-t/\tau_d},$$

where  $\tau_p$  and  $\tau_d$  correspond to the prompt and delayed fluorescence lifetimes. These lifetimes can be related to microscopic rate constants by solving the coupled differential equations under appropriate approximations [8]. In a steady state, the

photoluminescence quantum yield (PLQY) is given by

$$\Phi_{PL} = \frac{k_r N_s}{G_S + F_T} = \Phi_p + \Phi_d,$$

where  $\Phi_p$  and  $\Phi_d$  represents the prompt and delayed components. Analytical expressions for the delayed contribution  $\Phi_d$  provide an important link between experimentally measured delayed emission and theoretical RISC parameters[11].

At high excitation densities, typical in OLED operation, additional nonlinear processes such as triplet–triplet annihilation (TTA) and triplet–polaron quenching (TPQ) become relevant. These introduce quadratic loss terms, for example

$$-k_{TTA} N_T^2,$$

which complicate analytical treatments. Nevertheless, approximate solutions in the low-density regime remain useful for extracting parameters from transient photoluminescence experiments [12].

For device modeling, exciton dynamics must also be coupled to charge injection and recombination processes. Connecting microscopic kinetic rates to macroscopic quantities such as the external quantum efficiency (EQE) requires averaging over exciton formation statistics and optical outcoupling factors [12]. Although more detailed device models are discussed in the next chapter, this interplay highlights the motivation for a unified analytical description of exciton kinetics.

## 2.5 Thermodynamic and Quantum-Mechanical Basis of TADF

Thermally activated delayed fluorescence (TADF) can be understood from both a thermodynamic and quantum mechanical perspective. Thermodynamically, TADF relies on an activated transition between the singlet and triplet electronic manifolds, which differ in spin multiplicity. At thermal equilibrium, the relative populations of these states follow Boltzmann statistics:

$$\frac{N_S}{N_T} = \frac{g_S}{g_T} \exp\left(\frac{\Delta E_{ST}}{k_B T}\right),$$

where the degeneracy factors are  $g_s = 1$  for the singlet state and  $g_T = 3$  for the triplet state. This relation tells us how many singlet states are thermally populated relative to triplets at a given temperature. As the singlet–triplet energy gap  $\Delta E_{ST}$  becomes smaller, or as the temperature increases, it becomes easier for the system to repopulate the singlet state thermally.

However, equilibrium considerations alone do not determine whether TADF actually occurs. In practice, the key quantities are the kinetic rates of intersystem crossing (ISC) and reverse intersystem crossing (RISC), which dictate how quickly population can move between the singlet and triplet manifolds. These processes are formally spin-forbidden, but they become possible due to a combination of spin–orbit coupling (SOC) and vibronic coupling[9]. In purely organic molecules, SOC is usually weak because the constituent atoms are light, but vibronic coupling, the interaction between electronic and vibrational wavefunctions, can significantly enhance ISC and RISC by mixing charge-transfer (CT) and locally excited (LE) configurations[13].

The effective SOC matrix element that mediates RISC can be expressed schematically as

$$\langle S_1 | \hat{H}_{SO}^{eff} | T_1 \rangle = \sum_n \frac{\langle S_1 | \hat{H}_{SO} | T_n \rangle \langle T_n | \hat{H}_{vib} | T_1 \rangle}{E_{T_1} - E_{T_n}},$$

where  $\hat{H}_{SO}$  denotes the spin–orbit coupling operator and  $\hat{H}_{vib}$  describes vibronic interactions. Although this expression is difficult to evaluate analytically, it offers useful intuition: RISC becomes more efficient when higher-lying triplet states ( $T_n$ ) of different electronic character lie close enough in energy to mix with the CT-type ( $T_1$ ) state through vibronic coupling, while also providing a pathway for SOC to operate. This is why many TADF molecules are designed to achieve a careful balance between CT and LE character.

From a thermodynamic perspective, the RISC process follows an Arrhenius-type temperature dependence, with an activation energy typically close to  $\Delta E_{ST}$ .

Experimentally, this behavior is often revealed by plotting the delayed fluorescence lifetime or intensity as a function of inverse temperature. The resulting Arrhenius plot usually has a slope consistent with  $\Delta E_{ST}$ , providing a convenient experimental route for estimating the singlet–triplet gap without resorting to high-level electronic structure calculations.

In summary, TADF arises from a subtle but powerful interplay between thermodynamics and quantum mechanics. A small  $\Delta E_{ST}$  makes thermal up-conversion feasible, vibronic coupling mixes the relevant electronic characters needed for efficient ISC and RISC, and SOC, even if weak, provides the essential spin-flip mechanism. This combination enables efficient harvesting of triplet excitons and gives rise to the strong delayed fluorescence characteristic of TADF materials.

## 2.6 Molecular Factors Influencing Analytical Parameters

Even though this thesis focuses on analytical modeling rather than designing new molecules, it is still helpful to understand how certain structural features shape the parameters that go into those models.

**Donor–acceptor separation:** When the HOMO (donor) and the LUMO (acceptor) are farther apart, the exchange interaction  $J$  becomes smaller, which reduces the singlet–triplet gap ( $\Delta E_{ST} \approx 2J$ ) [14]. However, if the donor and acceptor become too separated, the orbital overlap drops and the radiative rate  $k_r$  decreases. Because of this trade, analytical models often treat  $\Delta E_{ST}$  and  $k_r$  as parameters that tend to vary in opposite directions.

**CT versus LE character:** Real TADF emitters are rarely pure charge transfer (CT) or purely locally excited (LE). They usually fall somewhere in between. A bit of LE character helps maintain oscillator strength, while CT character keeps  $\Delta E_{ST}$  small. Experiments indicate that efficient emitters typically show about 10–40% LE mixer. Analytical descriptions sometimes include a mixing coefficient to capture

how this balance influences the RISC prefactor  $A_{RISC}$  and the radiative rate  $k_r$ .

**Molecular rigidity and reorganization energy** Rigid molecular frameworks tend to suppress vibrational motion and reduce structural relaxation and after excitation. This lowers the reorganization energy  $\lambda$ , which plays an important role in the Marcus–Levich–Jortner expression for the RISC rate. Without going into full detail here, the key point is that a smaller  $\lambda$  generally increases  $k_{RISC}$  exponentially[15].

**Environment and host matrix effects:** The surrounding environment also affects the key parameters. Polar host materials can stabilize CT states and shift  $\Delta E_{ST}$  while aggregation and dielectric confinement can modify SOC strength and non-radiative decay rates. Analytical models usually incorporate these effects through effective medium parameters or empirical correction factors.

**Temperature dependence:** Because TADF materials can be affected thermally, temperature influences not only  $k_{RISC}$  but also the balance between radiative and non-radiative processes. Analytical treatments often use Arrhenius or Eyring-type expressions to describe how the delayed fluorescence yield changes with temperature[8].

Taken together, these molecular considerations help justify the typical parameter ranges used in analytical modeling: radiative rates  $k_r \sim 10^7 - 10^8 \text{ s}^{-1}$ , ISC rates  $k_{ISC} \sim 10^6 - 10^7 \text{ s}^{-1}$ , and RISC rates  $k_{RISC} \sim 10^3 - 10^6 \text{ s}^{-1}$  at room temperature [11]. Keeping these magnitudes in mind makes it easier to understand the emission kinetics and motivates the analytical models discussed later.

## 2.7 Analytical Treatments of RISC: Marcus and Marcus–Levich–Jortner Frameworks

A widely used analytical description of reverse intersystem crossing is based on Marcus theory, where RISC is treated as a thermally activated, non-adiabatic transition between two displaced harmonic potential energy surfaces. Within this picture,

the rate can be derived using Fermi’s Golden Rule and depends on the spin-orbit coupling between singlet and triplet states, the singlet-triplet energy gap, and nuclear reorganization energy [16]. The resulting expression captures the characteristic activated temperature dependence of RISC that is commonly observed in TADF materials.

While the standard Marcus theory assumes a classical treatment of nuclear motion, many organic emitters exhibit strong coupling to specific intramolecular vibrational modes. To account for this, the Marcus-Levich-Jortner (MJL) formulation extends the theory by explicitly including quantized high-frequency vibrations [17]. In this framework, RISC proceeds through a ladder of vibration-assisted transitions, each weighted by a Franck-Condon factor. This allows efficient spin conversion even when the purely classical activation barrier would be too large.

Together, these models provide a clear connection between molecular parameters—such as the reorganization energy  $\lambda$  (typically in the range of 0.1 - 0.3 eV), the singlet-triplet gap  $\Delta E_{ST}$ , and the effective spin-orbit coupling— and experimentally measured activation energies and temperature dependence. As a result, Marcus and MLJ theories have become standard tools for interpreting RISC kinetics and guiding the molecular design of efficient TADF emitters.

## 2.8 Density-Matrix and Master-Equation Approaches

A way to build an analytical picture of TADF is to look at it from the viewpoint of open quantum systems. In this framework, we do not follow the full molecular wavefunction but instead work with the reduced density matrix  $\rho$ , which captures the populations and coherence of the  $S_1-T_1$  manifold. Its time evolution is described by a Lindblad master equation:

$$\frac{d\rho}{dt} = -\frac{i}{\hbar}[H, \rho] + \sum_j \left( L_j \rho L_j^\dagger - \frac{1}{2} \{L_j^\dagger L_j, \rho\} \right),$$

where the Hamiltonian  $H$  includes any coherent mixing between  $S_1$  and  $T_1$ , typically represented by a coupling term  $V_{SO}$ , and the Lindblad operators  $L_j$  account for incoherent processes such as radiative decay, non-radiative decay, and ISC/RISC pathways [18].

This approach is useful because it treats coherent and incoherent effects within a single formalism. If, for example, the coupling between  $S_1$  and  $T_1$  were unusually strong or if vibrational motion produced long-lived coherence, the density matrix naturally reflects these features. In most organic TADF emitters, however, such coherence decay quickly. Under the secular approximation, where off-diagonal coherence terms vanish much faster than populations, the master equation greatly simplifies. In this limit, the full quantum description reduces to the classical rate equations commonly used in kinetic modeling. Although the density-matrix framework is mathematically heavier, it helps clarify when coherence plays a role and when it does not. Importantly, in the steady-state limit, the rate expressions that emerge from the master equation match the forms obtained from standard kinetic models, providing a consistent bridge between detailed open-quantum-system theory and practical analytical descriptions of ISC/RISC dynamics.

## 2.9 Analytical Expressions for Quantum Yield and Efficiency

Several studies have provided an overall photoluminescence quantum yield (PLQY) of TADF materials can be understood by expressing it in terms of the underlying decay rates that govern prompt and delayed emission. A commonly cited analytical form [19, 20] writes the PLQY as a combination of the radiative rate, non-radiative pathways, and the ISC/RISC cycle. The first part captures the prompt fluorescence contribution, while the second part accounts for how much triplet population can return to the singlet state and emit as delayed fluorescence. In other words, delayed fluorescence acts as an efficiency ‘recovery’ mechanism, enabling triplets that would

normally decay non-radiatively to contribute to overall light output.

In the OLED literature, this PLQY is often connected to the internal quantum efficiency (IQE), which is typically written in simplified form as

$$IQE = \Phi_{PL} \eta_{exc},$$

where  $\eta_{exc}$  is the exciton formation efficiency. Most reports assume  $\eta_{exc} \approx 1$  for high-quality devices, meaning almost all electron-hole pairs form excitons. Under these ideal conditions, the IQE is essentially limited by the photophysics of the emitter—namely, how effectively the material channels population through its radiative and RISC pathways.

However, the PLQY measured at low excitation levels does not always translate directly to device performance. Many experimental studies highlight that at high current densities, additional loss mechanisms come into play. Two frequently discussed processes are triplet-triplet annihilation (TTA) and triplet-polaron quenching (TOQ), which reduce the effective  $\Phi_{PL}$ . TTA scales approximately with the square of the triplet density,  $N_T^2$ , while TPQ depends on both the triplet and polaron densities,  $N_T N_P$  [21]. Analytical expressions incorporating these terms have been widely used to explain the roll-off in efficiency commonly observed in TADF OLEDs.

What makes these analytical forms valuable in the literature is that they provide simple, closed-form relationships connecting measurable quantities, such as decay lifetimes, activation energies, and rate constants, to macroscopic device metrics. This allows us to quickly interpret experimental data and compare the performance of different emitters without requiring detailed numerical simulations. As a result, these models have become standard tools for analyzing TADF behavior and for understanding how molecular photophysics translates into device-level efficiency.

## 2.10 Limitations and Open Problems in Analytical Descriptions

Even though analytical models are extremely useful for understanding TADF, they also come with some notable drawbacks. Several simplifications that make these models easy to use can also limit how accurately they reflect real materials and devices. Some of the main issues highlighted in the literature are the following:

**Oversimplified energy landscapes.** Most analytical treatments assume that  $S_1$  and  $T_1$  are each single, well-defined energy levels. In reality, organic emitters, especially in amorphous thin films, exhibit a whole distribution of vibrational sub-levels and conformational variation. These additional degrees of freedom can influence both ISC and RISC in ways that simple models do not capture.

**Neglect of environmental fluctuations.** Real solid-state hosts are not static. Their local dielectric environment fluctuates on picosecond timescales, and molecules can subtly reorient. These motions can cause small but important variations in  $\Delta E_{ST}$  and in the reorganization energy  $\lambda$ , making steady-state assumptions somewhat questionable in certain conditions [22].

**Interdependence of key parameters.** Analytical models often treat quantities like  $\Delta E_{ST}$ , the spin-orbit coupling strength  $V_{SO}$ , and  $\lambda$  as if they can be tuned independently. In practice, molecular modifications that shrink  $\Delta E_{ST}$  often weaken  $V_{SO}$  at the same time, or increase  $\lambda$ . These built-in trade-offs complicate molecular design and are not reflected in simple rate formulas [13].

**Coherent and non-Markovian effects.** When  $\Delta E_{ST}$  becomes very small, coherent coupling between singlet and triplet states can compete with the usual decay rates. In this regime, the assumption that ISC and RISC behave like memoryless, incoherent processes breaks down. Analytical descriptions for this borderline regime are still quite limited [23].

**Temperature and field dependence.** Most formulas assume that various

factors, such as RISC attempt frequencies or non-radiative decay rates, stay constant. Experiments, however, show that temperature and electric fields in devices can modify these rates in complicated ways, especially under operating conditions such as high operating currents/voltages, elevated device temperature, strong local fields etc..

Overall, these limitations point to the need for more flexible or hybrid approaches that link kinetic, quantum-mechanical, and statistical descriptions.

## 2.11 Summary of the Literature Review

Overall, the existing literature shows that thermally activated delayed fluorescence allows OLED emitters to make use of both singlet and triplet excitons by converting triplets back into singlets through thermal activation. Analytically, this behavior is usually described through a set of kinetic rate equations, where the different decay and conversion pathways are connected through temperature-dependent spin conversion processes. Key parameters, such as the reverse intersystem crossing rate, the singlet-triplet energy gap, and the reorganization energy play major roles in determining how efficiently a material splits its emission into prompt and delayed components. A range of analytical tools has been developed to capture these effects, including simple Arrhenius-type models, Marcus-Levich-Jortner theory, and even density-matrix approaches for more complex cases.

## 3 Relevant Models

Analytical models of thermally activated delayed fluorescence (TADF) aim to describe, in a clear mathematical way, how the excited states in organic emitters behave and produce light. While *ab initio* and density functional methods can provide quantities such as the singlet-triplet energy gap ( $\Delta E_{ST}$ ) or the strength of

spin-orbit coupling. But these numbers alone don't show how the molecule will actually emit light, how fast it will do so, or how the balance between different channels (radiative, non-radiative, ISC, RISC) plays out in real devices. Analytical models fill this gap. They sit between experiment and theory, helping us translate microscopic parameters into macroscopic observables like photoluminescence quantum yield, fluorescence lifetimes, or temperature dependence of delayed emission. This is useful in two ways:

For experimentalists: the model provides a map from measured decay curves (e.g., from time-resolved photoluminescence, TRPL) to underlying rate constants.

For theorists and device designers: one can quickly explore how changes to  $\Delta E_{ST}$ , reorganization energy  $\lambda$ , spin-orbit coupling  $V_{SO}$ , or molecular geometry affect overall performance—without running expensive simulations every time.

A good analytical description of TADF typically needs to:

- Keep track of how the population moves between the ground state, the singlet excited state, and the triplet state.
- Include all key processes: intersystem crossing (ISC), reverse intersystem crossing (RISC), and both radiative and non-radiative decay.
- Show clearly how the RISC rate depends on thermally activated parameters such as  $\Delta E_{ST}$  and the reorganization energy  $\lambda$ .

The following sections introduce the main analytical approaches used to capture these behaviors.

### 3.1 Kinetic Rate Equation Models

Almost every analytical description of thermally activated delayed fluorescence starts from the same basic idea: instead of tracking individual quantum states, we follow how populations of singlet and triplet excitons evolve in time. Transitions between

states are treated as stochastic processes, each characterized by a rate constant. This leads naturally to coupled rate equations.

Let  $N_S(t)$  and  $N_T(t)$  denote the populations of the lowest excited singlet  $S_1$  and triplet  $T_1$  states. If we ignore higher triplet levels for the moment, their time evolution is

$$\begin{aligned}\frac{dN_S}{dt} &= G_S - (k_r + k_{nr} + k_{ISC}) N_S + k_{RISC} N_T, \\ \frac{dN_T}{dt} &= G_T + k_{ISC} N_S - (k_T + k_{RISC}) N_T.\end{aligned}\quad (3.1)$$

Here,  $G_S$  and  $G_T$  are singlet and triplet generation rates (nonzero under continuous excitation).

$k_r$  is the radiative decay rate of  $S_1$ .

$k_{nr}$  is the non-radiative singlet decay rate.

$k_T$  is the intrinsic triplet decay rate, typically much smaller than all other rates.

These equations encode a simple but powerful picture. Once a singlet is created, it can emit light, decay non-radiatively, or convert into a triplet. Triplets, in turn, either slowly decay or convert back into singlets through RISC, where they get another chance to emit.

## Pulsed excitation and biexponential decay

Time-resolved photoluminescence experiments typically use a short laser pulse. After the pulse, there is no further exciton generation, so

$$G_S = G_T = 0 \quad \text{for } t > 0.$$

Solving Eq. (3.1) under these conditions gives a fluorescence signal consisting of two exponentials,

$$I(t) = A_p e^{-t/\tau_p} + A_d e^{-t/\tau_d}, \quad (3.2)$$

where the emission intensity is proportional to the singlet population,

$$I(t) = k_r N_S(t)$$

The fast, prompt component reflects what happens to singlets immediately after excitation. Its decay rate is approximately

$$\tau_p^{-1} \approx k_r + k_{nr} + k_{ISC}. \quad (3.3)$$

This timescale is set by all processes that directly depopulate  $S_1$ , and is therefore insensitive to the details of triplet dynamics.

The slower, delayed component arises from triplets that convert back into singlets before emitting. Its decay rate can be written as

$$\tau_d^{-1} \approx k_T + k_{RISC} \frac{k_r}{k_r + k_{nr} + k_{ISC}} \quad (3.4)$$

The second term reflects the fact that a triplet must first undergo RISC and then survive long enough in  $S_1$  to emit radiatively.

In simple terms: Prompt fluorescence tells us how singlets behave right away.

Delayed fluorescence tells us how efficiently and how quickly triplets recycle back into singlets.

Typical values are  $\tau_p \sim 10\text{--}100\text{ ns}$  and  $\tau_d \sim 1\text{--}1000\text{ }\mu\text{s}$ , clearly separating the processes in time.

## Steady state under continuous excitation

Under continuous optical or electrical excitation, the system reaches a steady state where the populations stop changing in time,

$$\frac{dN_S}{dt} = \frac{dN_T}{dt} = 0.$$

Solving Eq. (3.1) under these conditions gives closed-form expressions for  $N_S$  and  $N_T$  in terms of the rate constants and generation rates. These steady-state solutions are the starting point for analytical descriptions of OLED operation, linking microscopic exciton kinetics directly to measurable quantities such as brightness, efficiency, and roll-off.

### 3.2 Analytical Expressions for Quantum Yields and Lifetimes

One of the key numbers people care about in TADF materials in the photoluminescence quantum yield (PLQY). It basically tells us what fraction of excitons end up giving off light instead of getting lost along the way.

Starting from the usual definition,

$$\Phi_{PL} = \frac{k_r N_S}{k_r N_S + k_{nr} N_S + k_T N_T}. \quad (3.5)$$

If we plug in the steady-state solutions for the singlet and triplet populations, the expression unfolds into something a bit more detailed:

$$\Phi_{PL} = \frac{k_r}{k_r + k_{nr} + k_{ISC}} \left[ 1 + \frac{k_{ISC}}{k_r + k_{nr} + k_{ISC}} \frac{k_{RISC}}{k_T + k_{RISC}} \right] \quad (3.6)$$

The physical interpretation is surprisingly straightforward:

- The first term is just prompt fluorescence- singlets emitting before anything complicated happens.
- The second term is the delayed fluorescence, coming from triplets being recycled back into singlets through RISC.

Equation 3.6 also makes it clear why delayed fluorescence becomes strong only when RISC competes well with triplet decay:

$$k_{RISC} \gtrsim k_T.$$

In that regime, the triplets have a good chance of making it back to the singlet manifold and contributing to emission.

### Extracting rate constants from experiment

In practice, people often start from the measured prompt and delayed components of the emission. If we write the PLQY as the sum of prompt and delayed contributions,

we get

$$\Phi_p = \frac{A_p \tau_p}{A_p \tau_p + A_d \tau_d}, \quad \Phi_d = 1 - \Phi_p, \quad (3.7)$$

where  $A_p, \tau_p$  are the amplitude and lifetime of the prompt component, and  $A_d, \tau_d$  are the corresponding delayed values.

Once we are familiar with these, we can back out several of the microscopic rate constants in the model. This is the real power of these analytical expressions: they turn raw TRPL decay curves into quantities like  $k_{ISC}$ ,  $k_{RISC}$ , and the radiative and non-radiative rates. In other words, they help translate experiment into microscopic physics.

### 3.3 Temperature Dependence and Arrhenius Analysis

A very important feature of TADF is that the reverse intersystem crossing (RISC) is thermally activated. This means that triplet excitons need to climb up an energetic barrier, set mainly by the singlet-triplet gap  $\Delta E_{ST}$  and vibronic reorganization effects, before they can hop back into the singlet manifold.

A convenient way to model this is to assume an Arrhenius-type dependence,

$$k_{RISC}(T) = A_{RISC} \exp\left(-\frac{E_a}{k_B T}\right), \quad (3.8)$$

where  $A_{RISC}$  puts together spin-orbit coupling, vibronic coupling, etc., and  $E_a$  is an activation energy, usually close to  $\Delta E_{ST}$ .

#### How temperature affects the delayed component

As the temperature increases, more triplets get enough thermal energy to overcome the activation barrier. This naturally increases the population flow from  $T_1$  back to  $S_1$ , and therefore enhances the delayed fluorescence.

To see this more explicitly, recalling that the delayed intensity— at least in the simplest three-level model— scales approximately like

$$I_d(T) \propto \frac{k_{RISC}(T)}{k_T + k_{RISC}(T)}, \quad (3.9)$$

because only a fraction  $\frac{k_{RISC}}{k_T+k_{RISC}}$  of triplets successfully return to the singlet manifold before decaying non-radiatively or through phosphorescence.

Similarly, the delayed lifetime  $\tau_d(T)$  follows from the effective decay rate of the triplet reservoir. In the basic kinetic model,

$$\tau_d^{-1}(T) \approx k_T + k_{RISC}(T), \quad (3.10)$$

since these two processes are the main channels for depopulating the triplet state. This approximation is widely used in experimental fitting.

### Extracting activation energies: the Arrhenius plot

A common experimental trick is to isolate the RISC contribution in Eq. (3.10) by subtracting off the temperature-independent triplet decay:

$$k_{RISC}(T) = \tau_d^{-1}(T) - k_T.$$

Taking the logarithm of Eq. (3.8),

$$\ln k_{RISC}(T) = \ln A_{RISC} - \frac{E_a}{k_B} \frac{1}{T}$$

So if we plot

$$\ln\left(\frac{1}{\tau_d(T)} - k_T\right) \quad \text{vs.} \quad \frac{1}{T}, \quad (3.11)$$

we should get a straight line with slope

$$-\frac{E_a}{k_B}.$$

In real TADF molecules, the extracted  $E_a$  values typically lie between 0.05 and 0.25 eV, nicely matching known  $\Delta E_{ST}$  ranges. This is one of the experimental signatures of thermally activated triplet up-conversion.

## Low-temperature and high temperature limits

The model above behaves sensibly in both limiting regimes:

**Low temperature** ( $T \lesssim 150 \text{ K}$ ). The exponential suppression in Eq (3.8) makes

$$k_{RISC}(T) \rightarrow 0,$$

so nearly no triplets return to the singlet manifold. Delayed fluorescence fades out, and the emission becomes either phosphorescent or very weak.

**High temperature.** The RISC rate grows quickly:

$$k_{RISC}(T) \gg k_T,$$

and therefore the fraction in Eq. (3.9) approaches 1. Most triplets get recycled, delayed fluorescence becomes strong, and the total PLQY may rise substantially.

These simple temperature dependences are why Arrhenius-style analysis remains one of the most practical tools for characterizing TADF systems. Even though real molecules may deviate from a perfect three-level model, the Arrhenius treatment still provides clear physical intuition and direct experimental access to microscopic energy gaps.

### 3.4 Spin Statistical and Exciton-Formation Models

When a TADF material is placed inside an OLED, excitons are created electrically when electrons and holes recombine. In this situation, the first equation is simply: how many of the newly formed excitons are singlets and how many are triplets?

If we assume that the electron and hole spins are completely uncorrelated, then the possible spin-states of the electron-hole pair give a straightforward statistical ratio:

$$\eta_S : \eta_T = 1 : 3. \tag{3.12}$$

That is,

$$\eta_S = 0.25, \quad \eta_T = 0.75. \quad (3.13)$$

This "1-to-3 rule" is the standard starting point. However, real OLEDs often do not follow this exactly. Effects such as polaron-pair spin mixing, exchange interactions, or even asymmetric injection layers can bias the formation probabilities. Because of this, it's common to introduce an adjustable singlet-formation efficiency parameter  $\eta_{SF}$ , which scales the singlet probability:

$$\eta_S = 0.25 \eta_{SF} \quad \eta_T = 1 - \eta_S. \quad (3.14)$$

Here  $\eta_{SF} = 1$  returns the ideal 1:3 ratio. while  $\eta_{SF} > 1$  or  $\eta_{SF} < 1$  shifts the balance toward more or fewer singlets, respectively.

These formation fractions matter because they define the initial conditions for the rate-equation model of TADF under electrical excitation. Once excitons are created, TADF takes over: triplets can undergo RISC and eventually feed back into the singlet population.

Because both singlets and triplets can, directly or indirectly, generate photons, the internal quantum efficiency(IQE) can be written in a simple additive form:

$$\text{IQE} = \eta_S \Phi_p + \eta_T \Phi_d, \quad (3.15)$$

where  $\Phi_p$  is the prompt-fluorescence quantum yield, and  $\Phi_d$  is the delayed-fluorescence quantum yield.

In a highly efficient TADF system where RISC is fast, nearly all triplets eventually recycle into the singlet manifold. In that limit,  $\Phi_d \approx 1$  and therefore the IQE can approach unity- even though only  $\sim 25\%$  of excitons were singlets to begin with. This is one of the key reasons TADF can achieve very high device efficiencies without using heavy-metal dopants.

### 3.5 Marcus and Marcus-Levich-Jortner (MLJ) Analytical Treatments

A more microscopic description of reverse intersystem crossing (RISC) can be obtained by treating it as a thermally activated nonradiative transition between the triplet and singlet potential-energy surfaces. This process is mathematically analogous to an electron-transfer reaction, and its rate can therefore be described within the Marcus-type framework originally developed for charge transfer and later extended by Levich and Jortner to include discrete high-frequency vibrational modes.

The starting point is Fermi's Golden Rule applied to the transition  $T_1 \rightarrow S_1$ :

$$k_{RISC} = \frac{2\pi}{\hbar} |V_{SO}|^2 \rho(E), \quad (3.16)$$

where  $V_{SO}$  denotes the effective spin-orbit coupling (SOC) matrix element responsible for mixing the singlet and triplet manifolds, and  $\rho(E)$  is the Franck-Condon-weighted density of final vibrational states. The latter incorporates the overlap between vibrational wavefunctions on the two electronic surfaces.

#### Marcus Description

Assuming that the  $S_1$  and  $T_1$  potential energy surfaces are approximately parabolic and displaced along a nuclear coordinate by a reorganization energy  $\lambda$ , the density of states factor can be evaluated analytically. This yields the classical Marcus expression:

$$k_{RISC} = \frac{2\pi}{\hbar} |V_{SO}|^2 \frac{1}{\sqrt{4\pi\lambda k_B T}} \exp\left[-\frac{(\lambda + \Delta E_{ST})^2}{4\lambda k_B T}\right], \quad (3.17)$$

where  $\Delta E_{ST} = E_{S_1} - E_{T_1}$  is the singlet-triplet energy gap. The exponential factor encodes the thermally activated nature of RISC, while the prefactor combines the effects of SOC and nuclear reorganization. For typical donor-acceptor TADF emitters,  $\lambda$  often lies in the range 0.1 – 0.3 eV, so the magnitudes of  $\lambda$  and  $\Delta E_{ST}$  jointly determine whether RISC proceeds efficiently.

## Marcus–Levich–Jortner Refinement

Because Marcus theory treats nuclear motion classically, it becomes insufficient when high-frequency intramolecular modes play a significant role. To incorporate quantized vibrations, the Marcus–Levich–Jortner (MLJ) formulation introduces a vibrational mode of frequency  $\omega_m$  with Huang-Phys factor  $S_m$ . The resulting rate expression becomes a weighted sum over vibrational quanta:

$$k_{RISC} = \frac{2\pi}{\hbar} |V_{SO}|^2 \sum_{n=0}^{\infty} e^{-S_m} \frac{S_m^n}{n!} \frac{1}{\sqrt{4\pi\lambda k_B T}} \exp\left[-\frac{(\lambda + \Delta E_{ST} + n\hbar\omega_m)^2}{4\lambda k_B T}\right] \quad (3.18)$$

Each term in the sum corresponds to a transition assisted by the absorption or emission of  $n$  vibrational quanta. For moderate Huang-Phys factors  $S_m < 1$ , only a few terms contribute appreciably, and the series converges rapidly.

## Physical implications

The MLJ framework provides a direct connection between the experimentally measured temperature dependence of RISC and the underlying molecular parameters. In particular, plotting

$$\ln k_{RISC} \quad \text{versus} \quad \frac{1}{T}$$

yields an Arrhenius-like curve whose slope and curvature encode both the reorganization energy  $\lambda$  and the effective singlet–triplet gap  $\Delta E_{ST}$ .

Thus, Marcus and MLJ analyses offer a rigorous theoretical route for interpreting thermally activated delayed fluorescence in terms of SOC strength, vibrational structure, and nuclear reorganization.

## 3.6 Density Matrix and Quantum Master Equation Approaches

An alternative and more microscopic way to describe singlet–triplet dynamics is to treat the system explicitly as an open quantum system. In this picture, the lowest singlet and triplet excited states,  $S_1$  and  $T_1$ , form an effective two-level quantum

system that is weakly coupled to a vibrational environment. Rather than tracking only population, one follows the full reduced density matrix  $\rho$ , which contains both populations and quantum coherences.

The time evolution of  $\rho$  is governed by Lindblad-type quantum master equation,

$$\frac{d\rho}{dt} = -\frac{i}{\hbar}[H, \rho] + \sum_j \left( L_j \rho L_j^\dagger - \frac{1}{2} \{ L_j^\dagger L_j, \rho \} \right), \quad (3.19)$$

where the Hamiltonian  $H$  contains the electronic energies of  $S_1$  and  $T_1$  as well as their coherent spin-orbit coupling. The Lindblad operators  $L_j$  describe irreversible processes such as radiative decay, non-radiative relaxation, and dephasing caused by the environment.

In many TADF systems, environmental decoherence is relatively fast compared to the singlet-triplet interconversion time. Under this condition, the off-diagonal coherences in  $\rho$  decay rapidly and can be adiabatically eliminated. The remaining dynamics then reduce to effective population rate equations that closely resemble the phenomenological models introduced earlier, but with rate constants that now have a clear microscopic origin.

Within this framework, the RISC rate can be written in a form that mirrors Fermi's Golden Rule,

$$k_{RISC} = \frac{2|V_{SO}|^2}{\hbar^2} \int_0^\infty dt \langle e^{i(H_T - H_S)t/\hbar} \rangle, \quad (3.20)$$

where  $V_{SO}$  is the effective spin-orbit coupling matrix element,  $H_S$  and  $H_T$  are the nuclear Hamiltonian on the singlet and triplet potential-energy surfaces, and  $\langle \dots \rangle$  denotes a thermal average over phonon states. The time integral explicitly encodes how vibrational dynamics and energy fluctuations enable the otherwise spin-forbidden transition.

This formulation naturally connects to the Marcus and MLJ pictures discussed earlier. When the correlation time is short, the integral in Eq. (3.20) reduces to a classical or semiclassical expression equivalent to Marcus-type rates. When the

bath dynamics are slower or when the singlet–triplet gap  $\Delta E_{ST}$  becomes very small, coherent effects and memory (non-Markovian) effects can no longer be ignored, and the full quantum treatment becomes essential.

One advantage of the density-matrix approach is that it smoothly interpolates between incoherent hopping and partially coherent dynamics. This is particularly relevant for modern TADF emitters with extremely small  $\Delta E_{ST}$ , where coherent single–triplet mixing may persist over experimentally relevant timescales. Steady-state solutions of the master equation yield analytical expressions for singlet and triplet populations, emission intensities, and lifetimes, making direct contact with time-resolved photoluminescence experiments.

In this sense, quantum master equations provide a unifying framework: simple-rate equations emerge as a limiting case, while more subtle vibronic and coherence effects can be systematically included when needed.

### 3.7 Analytical Modeling of Device Efficiency

From a device point of view, the most important performance metric for an OLED is the external quantum efficiency (EQE). EQE tells us how efficiently injected electrical charges are ultimately converted into photons that actually escape the device. At its simplest level, EQE can be written as

$$EQE = \eta_{out} \eta_{exc} \Phi_{PL}, \quad (3.21)$$

where  $\eta_{out}$  is the optical out-coupling efficiency (typically around 0.2–0.3 for standard planar OLED architectures),  $\eta_{exc}$  is the efficiency with which injected electrons and holes form excitons, and  $\Phi_{PL}$  is the photoluminescence quantum yield of the emissive layer.

What makes analytical modeling useful is that  $\Phi_{PL}$  is not just a fitting parameter—it can be written explicitly in terms of microscopic rate constants. Substituting the

analytical expression derived earlier for  $\Phi_{PL}$  gives

$$EQE = \eta_{out} \eta_{ext} \frac{k_r}{k_r + k_{nr} + k_{RISC}} \left[ 1 + \frac{k_{ISC} k_{RISC}}{(k_T + k_{RISC})(k_r + k_{nr} + k_{ISC})} \right] \quad (3.22)$$

This expression makes the underlying physics quite transparent. The prefactor corresponds to prompt fluorescence from singlet excitons, while the term in square brackets captures the additional contribution coming from triplets that are recycled back into the singlet manifold through RISC. In the ideal TADF regime, where the reverse intersystem crossing rate  $k_{RISC}$  is large compared to the triplet decay rate  $k_T$ , triplet excitons are efficiently converted back into emissive singlets. As a result, both initially formed singlets and triplets can contribute to light emission, allowing EQE to approach its theoretical maximum.

At higher current densities, however, this ideal picture starts to break down. Additional loss mechanisms become important, particularly those involving interactions between excited states and charge carriers. Two of the most relevant processes are triplet–triplet annihilation (TTA) and triplet–polaron quenching (TPQ). Both processes reduce the steady-state triplet population and therefore suppress the delayed fluorescence component.

These effects can be included phenomenologically by adding nonlinear loss terms to the triplet rate equation,

$$\left( \frac{dN_T}{dt} \right)_{loss} = -k_{TTA} N_T^2 - k_{TPQ} N_T N_P, \quad (3.23)$$

where  $k_{TTA}$  and  $k_{TPQ}$  are the annihilation and quenching rate constants, respectively, and  $N_P$  is the polaron density.

Solving the steady-state rate equations with these additional terms leads to a reduction of the delayed emission at high excitation densities. When propagated through Eq (3.22), this results in a drop in EQE with increasing current, exactly the efficiency roll-off that is widely observed in TADF-based OLEDs. In this way, relatively simple analytical models provide a clear link between molecular-scale photophysics and practical device-level limitations.

### 3.8 Extended Analytical Models

#### Inclusion of Higher Triplet States $T_n$

In many TADF systems, the direct coupling between the lowest triplet  $T_1$  and singlet  $S_1$  is actually pretty weak. That means RISC doesn't happen efficiently through just  $T_1 \longleftrightarrow S_1$ . Luckily, higher-energy triplet states  $T_n$  can act as stepping stones, helping the system recycle triplets into singlets more efficiently.

We can capture this idea with a simple three-level model:  $T_1 \longleftrightarrow T_n \longleftrightarrow S_1$ . In this picture, the effective RISC rate can be written as:

$$k_{RISC}^{eff} = \frac{k_{T_1 T_n} k_{T_n S_1}}{k_{T_n T_1} + k_{T_n S_1} + k_{nr,n}}, \quad (3.24)$$

where:  $k_{T_1 T_n}$  is the vibrational up-conversion rate, essentially how quickly  $T_1$  can hop up to the higher triplet  $T_n$  through phonon interactions.

$k_{T_n S_1}$  is the spin-orbit coupling-assisted spin-flip rate, giving the probability for  $T_n \rightarrow S_1$ .

$k_{nr,n}$  accounts for non-radiative losses from  $T_n$

This simple formula explains why RISC can be much faster in molecules where a nearby  $T_n$  lies within  $\sim 0.1 eV$  of  $S_1$ . Physically, the system just climbs to the higher triplet and then flips to the singlet more easily than trying to hop straight from  $T_1$  to  $S_1$  [24, 5].

Intuitively, we can think of  $T_n$  as a shortcut or bridge: it's like taking a side path up a hill rather than trying to jump the entire distance in one go.

#### Triplet–Triplet Annihilation (TTA) and Triplet–Polaron Quenching (TPQ)

When the excitation intensity is high, we also need to account for nonlinear loss processes that cause the loss of triplets. Two main reasons are:

Triplet–Triplet annihilation (TTA)– two triplets collide, and one or both get lost.

Triplet–Polaron quenching (TPQ)– a triplet collides with a charge carrier (polaron) and gets quenched.

We can fold these into the steady-state triplet density  $N_T$  using the phenomenological loss equation:

$$\left(\frac{dN_T}{dt}\right)_{loss} = -k_{TTA}N_T^2 - k_{TPQ}N_TN_P, \quad (3.25)$$

where  $N_P$  is the polaron density.

For continuous generation at a rate  $G_T$ , the steady-state solution gives:

$$N_T = \frac{-k_{RISC} + \sqrt{-k_{RISC}^2 + 4k_{TTA}G_T}}{2k_{TTA}} \quad (3.26)$$

This near expression captures how the triplet population saturates nonlinearly at high generation rates. Physically, the more triplets we try to pack in, the faster they annihilate each other, so the delayed emission doesn't increase linearly with excitation; it bends over, giving the familiar roll-off in efficiency at high currents.

Even with these extra effects, the beauty of this approach is that it stays analytically tractable. We still get closed-form formulas connecting molecular rates  $k_{RISC}$ ,  $k_{TTA}$ ,  $k_{TPQ}$  to observables like triplet density and delayed fluorescence intensity, which makes it a very practical tool for understanding and predicting OLED behavior [25].

### 3.9 Summary

Analytical models of TADF bring together kinetics, thermodynamics, and quantum mechanics into a single, coherent picture. Starting from simple coupled rate equations, one can already obtain closed-form expressions for key observables such as excited-state lifetimes, photoluminescence quantum yields, and steady-state singlet and triplet populations.

Marcus and Marcus-Levich-Jortner theories go a step deeper by connecting the RISC rate to microscopic molecular parameters like the singlet-triplet energy gap  $\Delta E_{ST}$ , the reorganization energy  $\lambda$ , and the effective spin-orbit coupling  $V_{SO}$ . This makes it possible to translate experimental temperature dependences directly into concrete material design guidelines.

Master-equation and density-matrix approaches extend this framework further by explicitly accounting for interactions with the environment. These methods naturally include decoherence and non-Markovian effects, which become especially important in systems with very small singlet-triplet gaps.

Finally, extended analytical models that include higher-lying triplet states as intermediates, as well as nonlinear quenching processes, capture the efficiency roll-off observed at high excitation densities in real devices.

Taken together, these analytical approaches form a solid theoretical backbone for understanding TADF, linking molecular photophysics to device-level performance. They also set the stage for the analytical method developed in the following chapter of this thesis.

## 4 Generic Model and Results

The aim of this section is to develop an analytical kinetic description of thermally activated delayed fluorescence (TADF). While the phenomenology of prompt and delayed emission is well established experimentally, a clear connection between measured time-resolved photoluminescence (TRPL) signals and underlying microscopic rates requires an explicit solution of coupled population dynamics. In particular, experimentally observed decay components are often interpreted in such a way that the precise role of the individual transition rates remains implicit. An explicit solution of the coupled population dynamics is therefore required in order to relate measurable observables to the fundamental kinetic parameters of the system.

We begin with the three-state model involving the ground state  $S_0$ , the lowest excited singlet  $S_1$ , and the lowest excited triplet  $T_1$ . This model consists of all the defining features of TADF: intersystem crossing (ISC), reverse intersystem crossing (RISC), prompt fluorescence, and delayed fluorescence. After solving this model analytically, we extend the formalism to include higher excited singlet and triplets  $S_n$  and  $T_n$ . Basically, this extension does not introduce a fundamentally new theoretical framework. Instead, it is shown to be a natural generalization of the same linear algebraic structure already encountered in the three-state model. The additional states merely enlarge the dimensionality of the rate matrix, while the conceptual interpretation of its eigenvalues and eigenvectors remains unchanged.

Throughout this section, emphasis is placed on explicit algebraic steps, and a clear physical interpretation of each mathematical result. Approximations are introduced only when they can be justified physically, and their consequences are discussed explicitly. The goal is to provide an understanding of how thermally activated delayed fluorescence arises from the interplay of spin statistics, energy level alignment, and transition rates. In this way, the calculation section establishes a solid theoretical foundation for the analysis of experimental data and for the subsequent extension to more complex models.

## 4.1 Three-State Kinetic Model

We consider a molecular system described by three electronic states: the electronic ground state  $S_0$ , the lowest excited singlet state  $S_1$ , and the lowest excited triplet state  $T_1$ . Together, these states form the simplest set needed to describe the key processes involved in thermally activated delayed fluorescence.

The possible transitions between these states are summarized by a small number of elementary processes. From the excited singlet state  $S_1$ , the system can relax to the ground state  $S_0$  either through radiative decay (fluorescence) with  $k_{rS}$  or through

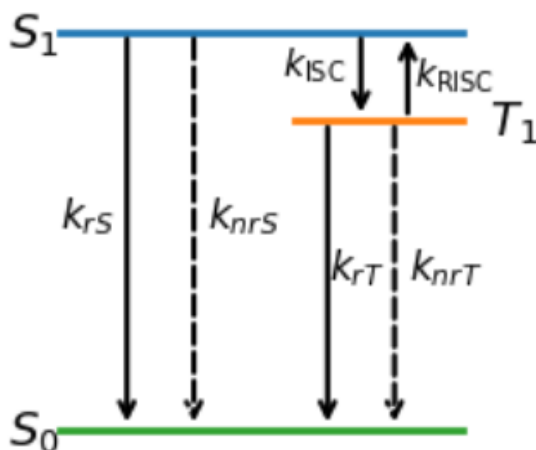


Figure 1. Three-state TADF model

non-radiative decay with rate  $k_{nrS}$ . Also, population can be transferred from  $S_1$  to the triplet state  $T_1$  via intersystem crossing (ISC), described by the rate  $k_{ISC}$ .

Population in the triplet state  $T_1$  can decay back to the ground state  $S_0$  through radiative decay (phosphorescence) with rate  $k_{rT}$  or through non-radiative decay with rate  $k_{nrT}$ . Alternatively, the triplet population may return to the singlet manifold through reverse intersystem crossing (RISC), which occurs at a rate  $k_{RISC}$  and is typically thermally activated.

Taken together, these processes define a closed kinetic scheme that captures the essential physics of TADF. Although the model is a minimal one, it already describes the appearance of both prompt fluorescence, arising from directly from  $S_1$ , and delayed fluorescence, coming from temporary population of  $T_1$  followed by RISC. As such, the three-state scheme provides a clear and intuitive starting point for the analytical treatment of TADF population dynamics.

To aid visualization, Fig.1 shows a schematic representation of the three-state kinetic model. The diagram highlights the three electronic states and the allowed transitions between them, with the corresponding rate constants.

## Mathematical description of three-state model

Let us define the total decay rates out of the excited states:

$$k_S \equiv k_{rS} + k_{nrS} + k_{ISC}, \quad (4.1)$$

$$k_T \equiv k_{rT} + k_{nrT} + k_{RISC} \quad (4.2)$$

These quantities represent the inverse lifetimes of  $S_1$  and  $T_1$ , respectively, when there is no coupling between the two excited manifolds.

External excitation processes are described by generation terms:

- $G_S$ : Population injected directly into  $S_1$ .
- $G_T$ : population infected directly into  $T_1$ .

In optical excitation experiments,  $G_T$  is usually negligible, whereas in electrically driven devices both terms are relevant.

Let  $S_0(t)$ ,  $S_1(t)$ , and  $T_1(t)$  denote the time-dependent populations of the three states. In the absence of generation and loss channels outside the model, the total population is conserved:

$$S_0(t) + S_1(t) + T_1(t) = N_{tot}$$

This constraint implies that only two of the three populations are dynamically independent. As it will become clear below, the non-trivial dynamics reside entirely in the excited-state subspace  $S_1, T_1$

The coupled rate equations governing the populations are

$$\frac{dS_1}{dt} = -k_S S_1(t) + k_{RISC} T_1(t) + G_S(t),$$

$$\frac{dT_1}{dt} = k_{ISC} S_1(t) - k_T T_1(t) + G_T(t),$$

$$\frac{dS_0}{dt} = (k_{rS} + k_{nrS}) S_1(t) + (k_{rT} + k_{nrT}) T_1(t) - G_S(t) - G_T(t)$$

Each term has a direct physical interpretation: loss terms describe decay out of a state, while gain terms represent population transfer from another state or external excitation.

Introducing the population vector

$$\vec{R}(t) = \begin{pmatrix} S_0(t) \\ S_1(t) \\ T_1(t) \end{pmatrix}$$

the rate equations can be written compactly as

$$\frac{d\vec{R}}{dt} = M \vec{R} + \vec{b}(t),$$

where

$$M = \begin{pmatrix} 0 & k_{rS} + k_{nrS} & k_{rT} + k_{nrT} \\ 0 & -k_S & k_{RISC} \\ 0 & k_{ISC} & -k_T \end{pmatrix}$$

and

$$\vec{b}(t) = \begin{pmatrix} -G_S(t) - G_T(t) \\ G_S(t) \\ G_T(t) \end{pmatrix}$$

Using population conservation, the ground-state population can always be reconstructed as

$$S_0(t) = N_{tot} - S_1(t) - T_1(t). \quad (4.3)$$

Therefore, the essential dynamics are governed by the reduced two-dimensional system

$$\frac{d}{dt} \begin{pmatrix} S_1 \\ T_1 \end{pmatrix} = M_2 \begin{pmatrix} S_1 \\ T_1 \end{pmatrix} \quad (4.4)$$

where the reduced rate matrix is

$$M_2 = \begin{pmatrix} -k_S & k_{RISC} \\ k_{ISC} & -k_T \end{pmatrix}$$

The excited-state dynamics are governed by the reduced matrix  $M_2$ . To find the decay models of the system, we solve the characteristic equation

$$\det(M_2 - \lambda I) = 0,$$

where  $I$  denotes the 2 x 2 identity matrix.

Explicitly, this reads

$$\det \begin{pmatrix} -k_S - \lambda & k_{RISC} \\ k_{ISC} & k_T - \lambda \end{pmatrix} = 0$$

which expands to

$$(-k_S - \lambda)(-k_T - \lambda) - k_{ISC}k_{RISC} = 0.$$

Multiplying out, we obtain

$$\lambda^2 + (k_S + k_T)\lambda + k_S k_T - k_{ISC}k_{RISC} = 0.$$

This is a standard quadratic equation in  $\lambda$ . This equation has two solutions, corresponding to the two independent decay modes of the coupled  $(S_1, T_1)$  system.

Using the quadratic formula, we obtain the eigenvalues:

$$\lambda_{1,2} = -\frac{k_S + k_T}{2} \pm \frac{1}{2}\sqrt{(k_S - k_T)^2 + 4k_{ISC}k_{RISC}}.$$

Several important physical conclusions follow immediately from this expression. First, both eigenvalues are negative, ensuring dynamical stability and decay of the excited-state populations. Second, the appearance of the difference  $(k_S - k_T)^2$ , rather than the sum, reflects the competition between singlet and triplet decay channels. In the absence of coupling between the two manifolds  $k_{ISC} = k_{RISC} = 0$ , the square

root reduces to  $|k_S - k_T|$ , and the eigenvalues simply reproduce the independent decay rates  $-k_S$  and  $-k_T$ .

When intersystem crossing and reverse intersystem crossing are present, the term  $4k_{ISC}k_{RISC}$  mixes the singlet and triplet dynamics, leading to two hybrid decay modes.

These eigenvalues directly correspond to the prompt and delayed fluorescence timescales observed in TRPL experiments.

Having obtained the eigenvalues of the reduced excited-state rate matrix  $M_2$ , we now determine the corresponding eigenvectors explicitly and analyze their physical interpretation. While the eigenvalues control the decay time scales of the system, the eigenvectors encode the relative singlet and triplet populations associated with each decay mode and are therefore essential for understanding the origin of prompt and delayed fluorescence. For each eigenvalue  $\lambda$ , the corresponding eigenvector

$$v_i = \begin{pmatrix} v_S \\ v_T \end{pmatrix}$$

satisfies

$$(M_2 - \lambda_i I)v_i = 0.$$

Explicitly,

$$\begin{pmatrix} -k_S - \lambda_i & k_{RISC} \\ k_{ISC} & -k_T - \lambda_i \end{pmatrix} \begin{pmatrix} v_S \\ v_T \end{pmatrix} = 0.$$

The eigenvalue equation therefore, corresponds to the coupled system of linear equation

$$(-k_S - \lambda_i)v_S^i + k_{RISC}v_T^i = 0 \tag{4.5}$$

$$k_{ISC}v_S^i + (-k_T - \lambda_i)v_T^i = 0 \tag{4.6}$$

Since  $\lambda_i$  satisfies the characteristic equation

$$(\lambda_i + k_S)(\lambda_i + k_T) - k_{ISC}k_{RISC} = 0,$$

the determinant of  $M_2 - \lambda_i I$  vanishes, implying that Eqs.(4.5) and (4.6) are linearly dependent. Therefore, either equation may be used to determine the eigenvector up to an arbitrary normalization constant.

Let us proceed using the first equation, Eq. (4.5). From this equation we get

$$\frac{v_T^i}{v_S^i} = \frac{k_S + \lambda_i}{k_{RISC}}.$$

Because the eigenvectors are defined only up to an overall multiplicative factor, we are free to choose a convenient normalization. Choosing

$$v_S^i = 1,$$

the eigenvector associated with  $\lambda_i$  takes the explicit form

$$\vec{v}_i = \begin{pmatrix} 1 \\ \alpha_i \end{pmatrix}, \quad \alpha_i \equiv \frac{k_S + \lambda_i}{k_{RISC}}.$$

It is instructive to verify explicitly that this eigenvector also satisfies the second equation. Substituting  $v_S^i = 1$  and  $v_T^i = \alpha_i$  Eq.(4.6) gives

$$k_{ISC} + (-k_T - \lambda_i)\alpha_i = 0.$$

Using the definition of  $\alpha_i$  and the characteristic equation, this condition is satisfied identically, confirming the internal consistency of the solution.

From a physical point of view, each eigenvector corresponds to a decay mode in which the populations of  $S_1$  and  $T_1$  change together with a fixed ratio. The parameter  $\alpha_i$  therefore measures how much triplet character that particular mode has.

For the fast-decaying mode,  $|\alpha_i|$  is usually small. This means the dynamics are mainly governed by the singlet population, which results in prompt fluorescence.

In contrast, the slow-decaying mode has a much larger  $|\alpha_i|$ , indicating a significant contribution from the triplet state. This mode is responsible for delayed

fluorescence, as population stored in  $T_1$  is gradually transferred back to  $S_1$  through RISC.

In this way, the eigenvectors offer a clear physical interpretation of the rate equations, directly linking their mathematical structure to the experimentally observed separation between prompt and delayed emission in TADF systems.

With the eigenvalues  $\lambda_1$  and  $\lambda_2$  and corresponding eigenvectors  $v_1$  and  $v_2$  determined, the general solution for the excited-state populations can be expressed as a linear combination of the eigenmodes:

$$\begin{pmatrix} S_1(t) \\ T_1(t) \end{pmatrix} = c_1 v_1 e^{\lambda_1 t} + c_2 v_2 e^{\lambda_2 t}.$$

Explicitly, this reads

$$S_1(t) = c_1 e^{\lambda_1 t} + c_2 e^{\lambda_2 t}, \quad T_1(t) = \alpha_1 c_1 e^{\lambda_1 t} + \alpha_2 c_2 e^{\lambda_2 t}$$

where  $\alpha_i(k_S + \lambda_i)/k_{RISC}$  defines the singlet-triplet ratio for each mode.

The coefficients  $c_1$  and  $c_2$  are fixed by the initial populations  $S_1(0) = S_1^0$  and  $T_1(0) = T_1^0$ . Solving the linear system

$$c_1 + c_2 = S_1^0,$$

$$\alpha_1 c_1 + \alpha_2 c_2 = T_1^0,$$

we obtain,

$$c_1 = \frac{S_1^0 \alpha_2 - T_1^0}{\alpha_2 - \alpha_1}, \quad c_2 = -N_0 \frac{\alpha_1}{\alpha_2 - \alpha_1}.$$

Substituting back gives

$$S_1(t) = N_0 \left( \frac{\alpha_2 e^{\lambda_1 t} - \alpha_1 e^{\lambda_2 t}}{\alpha_2 - \alpha_1} \right), \quad T_1(t) = N_0 \left( \frac{\alpha_1 \alpha_2 (e^{\lambda_1 t} - e^{\lambda_2 t})}{\alpha_2 - \alpha_1} \right)$$

These expressions clearly show that the dynamics are a sum of the two exponential contributions, corresponding to the prompt and delayed modes.

$c_1$  and  $c_2$  quantify the initial weighting of each decay channel. The fast mode contributes primarily to the initial, singlet-dominated emission, while the slow mode governs the delayed fluorescence mediated by triplet population. This decomposition also gives a direct connection to TRPL fitting, where bi-exponential decay constants are routinely extracted from experimental traces.

The three-state model is particularly effective because it captures the essential features of TADF while remaining analytically traceable. Its validity relies on the following condition:

**Rapid relaxation of higher excited states:** Any higher states  $S_n$  or  $T_n$ , populated during excitation relax quickly into  $S_1$  or  $T_1$ , so that their dynamics can be effectively neglected in the first approximation.

**Dominance of the lowest triplet manifold:** Only  $T_1$  participates significantly in delayed fluorescence, that is caused by RISC, higher triplet states contribution is negligible.

**No significant multi-excitonic effects:** The model assumes isolated single excitations per molecule; exciton-exciton annihilation or higher-order processes are ignored.

The model begins to fail when higher-level singlet or triplet states are long-lived or directly involved in emission, or when multiple triplet states are populated under strong excitation. In these cases, a natural generalization to  $S_m$  and  $T_n$  levels is required, as will be discussed in the next section.

## 4.2 Extension to Higher Excited States

In order to construct a truly generic kinetic description of thermally activated delayed fluorescence, it is necessary to move beyond minimal three-level model and explicitly account for the presence of multiple singlet and triplet excited states. Organic molecules generally possess a dense manifold of electronically excited states,

and although many of these relax rapidly, they can play an important indirect role in determining intersystem crossing, reverse intersystem crossing, and delayed emission dynamics.

In this section, we therefore formulate a general rate-equation model that includes an arbitrary number of singlet excited states  $S_m$  and triplet excited states  $T_n$ , and we derive the corresponding matrix representation of the population dynamics. This formulation naturally reduces to commonly used models in appropriate limits, while retaining the flexibility to describe more complex photophysical scenarios.

## Mathematical description for the extended system

Let us consider a molecular system described by the electronic states

$$S_0, \quad S_1, \dots, S_M, \quad T_1, \dots, T_N,$$

where  $S_0$  denotes the electronic ground state,  $S_m$  the  $m$ -th singlet excited state, and  $T_n$  the  $n$ -th triplet excited state.

The corresponding population vector is defined as

$$\vec{R}(t) = \begin{pmatrix} S_0(t) \\ S_1(t) \\ \vdots \\ S_M(t) \\ T_1(t) \\ \vdots \\ T_N(t) \end{pmatrix}.$$

Population is conserved at all times,

$$S_0(t) + \sum_{m=1}^M S_m(t) + \sum_{n=1}^N T_n(t) = N_{tot},$$

where  $N_{tot}$  is the total number of excitations in the system.

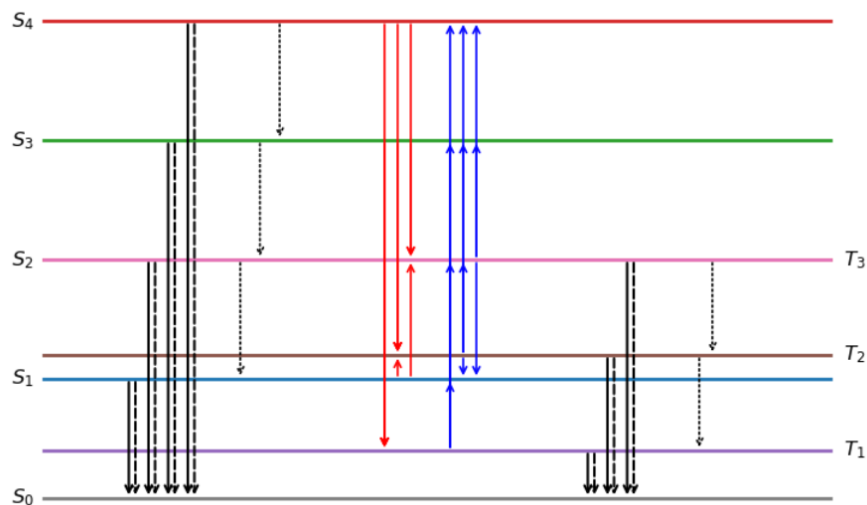


Figure 2. Schematic diagram for higher-level model

### Elementary processes and physical assumptions:

All population transfer processes are treated within a first-order kinetic approximation, which is well justified for incoherent excited-state dynamics in organic semiconductors.

Fig. 2 gives an idea about the population change in higher-lying states.

#### Singlet-singlet relaxation

Higher singlet states typically relax rapidly toward lower-lying singlets through internal conversion,

$$S_m \rightarrow S_{m-1}, \quad m \geq 2,$$

with rates  $k_{m,m-1}^S$ . These processes are usually fast compared to radiative decay and spin-flip processes, reflecting strong vibronic coupling within the singlet manifold. Thermally activated back-transfer  $S_{m-1} \rightarrow S_m$  may occur if the energy gap is sufficiently small, but is neglected here for clarity.

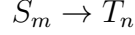
#### Singlet decay

Each singlet excited state may decay to the ground state via radiative or non-radiative channels, characterized by rate  $k_m^r$  and  $k_m^{nr}$ , respectively. In accordance

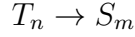
with Kasha's rule, radiative emission is typically dominated by the lowest singlet state, but higher singlets are retained here for generality.

### Intersystem crossing and reverse intersystem crossing

Spin-forbidden transitions between singlet and triplet manifolds are described by intersystem crossing (ISC)



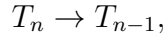
with rates  $k_{mn}^{ISC}$ , and reverse intersystem crossing (RISC)



with rates  $k_{nm}^{RISC}$ . In realistic TADF systems these processes are often mediated by vibronic and spin-orbit coupling and may involve higher-lying triplet states rather than a direct  $S_1 \leftrightarrow T_1$  transition.

### Triplet relaxation

Triplet states undergo internal conversion toward the lowest triplet



with rates  $k_{n,n-1}^T$ , as well as radiative (phosphorescent) and non-radiative decay with rates  $k_n^{rt}$  and  $k_n^{nrT}$ . In most purely organic TADF materials, phosphorescence is weak and non-radiative decay dominates.

### Rate equations

With these processes defined, the population dynamics follow directly from balance equations. The ground-state population changes due to decay from excited states and external excitation:

$$\frac{dS_0}{dt} = \sum_{m=1}^M (k_m^r + k_m^{nr}) S_m + \sum_{n=1}^N (k_n^{rT} + k_n^{nrT}) T_n - G(t),$$

where  $G(t)$  represents the total excitation rate.

For  $m = 1, \dots, M$ , the singlet excited states are

$$\frac{dS_m}{dt} = k_{m+1,m}^S S_{m+1} - k_{m,m-1}^S S_m - (k_m^r + k_m^{nr}) S_m - \sum_{n=1}^N k_{mn}^{ISC} S_m + \sum_{n=1}^N k_{nm}^{RISC} T_n + G_m(t).$$

Here,  $G_m(t)$  allows for state-selective excitation.

Similarly, for  $n = 1, \dots, N$ , the triplet excited states are

$$\frac{dT_n}{dt} = k_{n+1,n}^T T_{n+1} - k_{n,n-1}^T T_n - (k_n^{rT} + k_n^{nrT}) T_n + \sum_{m=1}^M k_{mn}^{ISC} S_m - \sum_{m=1}^M k_{nm}^{RISC} T_n$$

For compactness and analytical tractability, it is convenient to write the excited-state dynamics in matrix form. Defining the reduced population vector

$$\vec{r}(t) = \begin{pmatrix} S_1(t) \\ \vdots \\ S_M(t) \\ T_1(t) \\ \vdots \\ T_N(t) \end{pmatrix},$$

the rate equations can be written as

$$\frac{d}{dt} \vec{r}(t) = M_{ex} \vec{r}(t) + \vec{g}(t),$$

where  $\vec{g}(t)$  contains all excitation terms.

The kinetic matrix naturally separates into singlet, triplet, and coupling blocks,

$$M_{ex} = \begin{pmatrix} M_S & M_{ST} \\ M_{TS} & M_T \end{pmatrix}.$$

The singlet block  $M_S$  contains internal conversion and decay within the singlet manifold, the triplet block  $M_T$  describes relaxation within the triplet manifold, and the off diagonal blocks  $M_{ST}$  and  $M_{TS}$  encode ISC and RISC processes. This block structure makes explicit how singlet and triplet dynamics are coupled.

### Formal solution and decay modes:

For pulsed excitation,  $\vec{g}(t > 0) = 0$ , the formal solution is

$$\vec{r}(t) = e^{M_{ex}t} \vec{r}(0).$$

The time evolution is therefore governed by the eigenvalue problem

$$\det(M_{ex} - \lambda I) = 0,$$

yielding  $M + N$  decay rates. Each eigenvalue corresponds to a distinct relaxation mode, including prompt fluorescence, delayed fluorescence, and long-lived triplet storage.

### **Reduction to effective models**

Although the full formulation is general, it is often useful to reduce the system by exploiting the separation of timescales. Internal conversion within singlet and triplet manifolds is typically much faster than ISC and RISC allowing higher excited states to be adiabatically eliminated. In this way, the present framework reduces systematically to commonly used three- and four-level TADF models, while providing a clear physical interpretation of the resulting effective rates.

In summary, this formulation provides a unified kinetic description of TADF that explicitly includes multiple singlet and triplet levels. It retains sufficient generality to describe complex molecular systems, while remaining manageable to analytical treatment and systematic reduction.

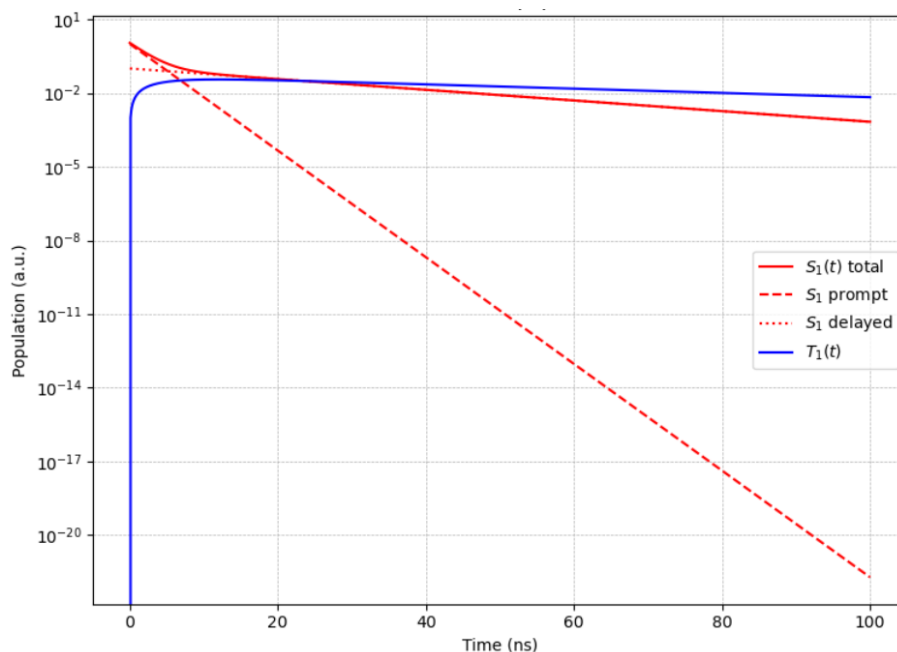
## **4.3 Results**

This chapter presents the main results obtained from the kinetic modeling of thermally activated fluorescence (TADF). The results are organized in a way that mirrors the theoretical development of the thesis. First the key outcomes of the conventional three-state model is summarized, and then the additional physical insights gained from the extended multi-state formulation is discussed. Throughout this chapter, the emphasis is placed on the physical interpretation of the results and their relevance for realistic TADF systems, rather than on mathematical derivations.

## Results of the Three-State TADF Model

The three-state model, consisting of the ground state  $S_0$ , the lowest singlet excited state  $S_1$ , and the lowest triplet excited state  $T_1$ , provides a minimal yet instructive description of TADF dynamics. Solving the coupled rate equations yields two distinct characteristic timescales in the excited-state population dynamics.

The first timescale corresponds to prompt fluorescence, mainly driven by the radiative and non-radiative decay of  $S_1$ . This shows up as a rapid exponential drop in emission intensity and dominates the early response right after excitation. How much of the population goes into the triplet state before emitting light depends on the intersystem crossing rate  $k_{RISC}$ .



The figure shows the time evolution of the excited-state populations. The  $S_1$  population exhibits a fast prompt decay followed by a slower delayed component, while the  $T_1$  population rises more slowly and decays on a longer timescale.

The second timescale comes from delayed fluorescence, which happens when triplet excitons are thermally converted back to the singlet state through RISC. This delayed emission lasts much longer, reflecting the slow decay of  $T_1$ . The effective

rate of delayed fluorescence depends on both the RISC rate  $k_{RISC}$  and the intrinsic triplet decay processes.

A key takeaway from the model is how the delayed fluorescence contributes to the overall emission. The contribution grows quickly as the energy gap between  $S_1$  and  $T_1$  gets smaller, which aligns with the thermal activation behind RISC. This explains an important design rule for TADF emitters: to efficiently harvest triplet excitons, we need both a small singlet-triplet energy gap and strong enough spin-orbit coupling.

However, the three-state model also has its limits. It assumes that all singlet-triplet population transfer happens only through  $S_1$  and  $T_1$ , ignoring the role of higher excited states. In real molecules, this is not always the case, so the model is simplification rather than a complete picture.

## Emergence of Additional Timescales in the Extended Model

When the model is extended to include several singlet and triplet excited states, the population dynamics become noticeably richer. One of the most obvious changes is that the system no longer evolves with just two characteristic timescales, as in the three-state picture. Instead, multiple decay components naturally appear.

By diagonalizing the full kinetic matrix, a clear hierarchy of processes emerges. Fast modes are associated with relaxation within the singlet or triplet manifolds, intermediate modes reflect intersystem crossing between them, and the slowest modes correspond to the long-lived decay of triplet populations. As a result, the emission intensity typically follows a multi-exponential decay, even without invoking energetic disorder or spatial inhomogeneity.

Higher-lying triplet states play a particularly important role by opening up additional pathways for reverse intersystem crossing. Rather than relying on a singlet  $T_1 \rightarrow S_1$  channel, population can move through several triplet levels before returning

to the singlet manifold. This redistribution increases the overall likelihood of RISC and can boost the delayed fluorescence yield, without requiring an unrealistically strong direct coupling between  $T_1$  and  $S_1$ .

## **Role of Internal Conversion within Singlet and Triplet Manifolds**

A key insight from the extended model is how important fast internal conversion is within both the singlet and triplet manifolds. When relaxation within a given manifold happens much faster than intersystem crossing, higher excited states never build up much population. Even so, they still affect the dynamics indirectly by shaping how population flows through the system.

In this limit, the extended model effectively collapses to a simpler, low-dimensional description with modified or renormalized, rate constants. Importantly, these effective rates are not universal: they depend on how many excited states are included in the model and on how closely spaced they are in energy. This offers a straightforward physical explanation for why RISC rates extracted from experiments can differ substantially between otherwise similar materials, even when their  $S_1 - T_1$  energy gaps are nearly the same.

## **Comparison Between the Three-State and Extended Models**

Comparing the three-state and extended models helps clarify when the simple picture is enough and when it starts to break down. If higher excited states are well separated in energy and relax very quickly, the three-state model does a good job of capturing the main features of the emission dynamics.

The situation changes when higher triplet states lie close in energy to the lowest singlet or take part directly in spin-orbit-assisted transitions. In these cases, the three-state model tends to underestimate the delayed fluorescence contribution. The

extended model shows that higher-lying states can serve as intermediate reservoirs that make triplet harvesting more efficient, even when the direct  $T_1 \rightarrow S_1$  reverse intersystem crossing rate is small.

## Implications for Molecular Design of TADF Emitters

From a materials design point of view, these results show that improving TADF performance is not just about minimizing the  $S_1 - T_1$  energy gap. Instead, the full excited-state landscape matters. Having several closely spaced triplet states, along with effective coupling between triplet and singlet states, can significantly boost the efficiency of delayed fluorescence.

The extended model provides a natural way to understand experimental results that do not fit neatly into simple three-state kinetics. More importantly, it points toward design strategies that focus on shaping the overall excited-state manifold, rather than tuning individual energy levels in isolation.

## Summary of Key Results

To summarize, the main findings of this thesis are:

- The three-state model captures the essential physics of TADF and naturally explains the presence of both prompt and delayed fluorescence.
- Extending the model to include multiple excited states reveals additional decay pathways and timescales that are not visible in minimal descriptions.
- Higher-lying singlet and triplet states can significantly enhance delayed fluorescence by opening up alternative routes for reverse intersystem crossing.
- The effective rates governing TADF depend on the structure of the entire excited-state manifold, not just the lowest singlet and triplet states.

- Overall, the extended framework provides a more realistic and flexible description of TADF in complex organic molecules.

## 5 Conclusion

This thesis presents a theoretical study of thermally activated delayed fluorescence with the goal of understanding how excited-state populations evolve in systems involving coupled singlet and triplet states. The work begins with simple models and gradually extends to more realistic descriptions that include multiple singlet and triplet levels. This progression makes it easier to isolate the key physical processes behind TADF and to see how they influence the observed emission dynamics.

Analytical solutions to the rate equations were obtained for both the standard three-level TADF model and its extended versions. These solutions offer a clear picture of how populations move between singlet and triplet states over time, and they directly illustrate the delayed repopulation of the emissive singlet state that gives rise to delayed fluorescence. Seeing this behavior emerge naturally from the analytical expressions helps build intuition and confirms that the essential physics is captured by the model.

By allowing higher-lying excited states, the extended models show how population redistribution across multiple levels can affect the overall dynamics without changing the basic mechanism of TADF. In particular, higher triplet states can act as temporary reservoirs that modify effective rates and timescales, which is likely to be important in real organic emitters where many excited states are closely spaced in energy.

Overall, this work provides a flexible analytical framework for describing TADF dynamics beyond the simplest models. The results should be useful for interpreting time-resolved photoluminescence measurements and for developing more refined theoretical descriptions in the future. Possible extensions include incorporating

temperature-dependent rates, vibrational effects, or energetic disorder, which would allow the model to connect more directly with experimental systems and material-specific behavior.

## Use of AI in thesis

I have used AI assisted tools for language and style improvement as well as idea clarification. I have used Grammarly, Gemini 3, and ChatGPT 4.1. Specifically, Grammarly was used for grammar, spelling and clarity suggestions. ChatGPT and Gemini were used to find relevant papers, and to support understanding of general concepts.

## References

- [1] Ching W Tang and Steven A VanSlyke. “Organic electroluminescent diodes”. In: *Applied physics letters* 51.12 (1987), pp. 913–915.
- [2] Martin Pope and Charlese E Swenberg. *Electronic processes in organic crystals and polymers*. Oxford University Press, 1999.
- [3] Richard H Friend et al. “Electroluminescence in conjugated polymers”. In: *Nature* 397.6715 (1999), pp. 121–128.
- [4] MA Baldo, MI E ThompSON, and SR Forrest. “High-efficiency fluorescent organic light-emitting devices using a phosphorescent sensitizer”. In: *Nature* 403.6771 (2000), pp. 750–753.
- [5] Hiroki Uoyama et al. “Highly efficient organic light-emitting diodes from delayed fluorescence”. In: *Nature* 492.7428 (2012), pp. 234–238.
- [6] Hajime Nakanotani et al. “High-efficiency organic light-emitting diodes with fluorescent emitters”. In: *Nature communications* 5.1 (2014), p. 4016.
- [7] Shuzo Hirata. “Recent advances in materials with room-temperature phosphorescence: photophysics for triplet exciton stabilization”. In: *Advanced Optical Materials* 5.17 (2017), p. 1700116.
- [8] Fernando B Dias, Thomas J Penfold, and Andrew P Monkman. “Photophysics of thermally activated delayed fluorescence molecules”. In: *Methods and applications in fluorescence* 5.1 (2017), p. 012001.
- [9] TJ Penfold, FB Dias, and Andrew P Monkman. “The theory of thermally activated delayed fluorescence for organic light emitting diodes”. In: *Chemical communications* 54.32 (2018), pp. 3926–3935.
- [10] Hiroki Noda, Hajime Nakanotani, and Chihaya Adachi. “Excited state engineering for efficient reverse intersystem crossing”. In: *Science Advances* 4.6 (2018), eaa06910.
- [11] Marc K Etherington et al. “Revealing the spin–vibronic coupling mechanism of thermally activated delayed fluorescence”. In: *Nature Communications* 7.1 (2016), p. 13680.
- [12] Kenichi Goushi and Chihaya Adachi. “Efficient organic light-emitting diodes through up-conversion from triplet to singlet excited states of exciplexes”. In: *Applied Physics Letters* 101.2 (2012).
- [13] Jamie Gibson, Andrew P Monkman, and Thomas J Penfold. “The importance of vibronic coupling for efficient reverse intersystem crossing in thermally activated delayed fluorescence molecules”. In: *ChemPhysChem* 17.19 (2016), pp. 2956–2961.
- [14] Xian-Kai Chen, Dongwook Kim, and Jean-Luc Brédas. “Thermally activated delayed fluorescence (TADF) path toward efficient electroluminescence in purely organic materials: molecular level insight”. In: *Accounts of Chemical Research* 51.9 (2018), pp. 2215–2224.

- [15] Seung-Je Woo and Jang-Joo Kim. “TD-DFT and experimental methods for unraveling the energy distribution of charge-transfer triplet/singlet states of a tadf molecule in a frozen matrix”. In: *The Journal of Physical Chemistry A* 125.5 (2021), pp. 1234–1242.
- [16] Rudolph A Marcus. “On the theory of oxidation-reduction reactions involving electron transfer. I”. In: *The Journal of chemical physics* 24.5 (1956), pp. 966–978.
- [17] Jens Ulstrup and Joshua Jortner. “The effect of intramolecular quantum modes on free energy relationships for electron transfer reactions”. In: *The Journal of chemical physics* 63.10 (1975), pp. 4358–4368.
- [18] Heinz-Peter Breuer and Francesco Petruccione. *The theory of open quantum systems*. OUP Oxford, 2002.
- [19] Ayataka Endo et al. “Efficient up-conversion of triplet excitons into a singlet state and its application for organic light emitting diodes”. In: *Applied Physics Letters* 98.8 (2011).
- [20] Yun Hu et al. “Exciplex-Based Organic Light-Emitting Diodes with Near-Infrared Emission”. In: *Advanced Optical Materials* 8.7 (2020), p. 1901917.
- [21] Sebastian Scholz et al. “Degradation mechanisms and reactions in organic light-emitting devices”. In: *Chemical reviews* 115.16 (2015), pp. 8449–8503.
- [22] Stavros Athanasopoulos et al. “Exciton diffusion in energetically disordered organic materials”. In: *Physical Review B—Condensed Matter and Materials Physics* 80.19 (2009), p. 195209.
- [23] Colin Y Kim et al. “The chloroalkaloid (-)-acutumine is biosynthesized via a Fe (II)-and 2-oxoglutarate-dependent halogenase in Menispermaceae plants”. In: *Nature Communications* 11.1 (2020), p. 1867.
- [24] Ayataka Endo et al. “Thermally activated delayed fluorescence from Sn4+-porphyrin complexes and their application to organic light-emitting diodes—A novel mechanism for electroluminescence”. In: *Advanced Materials* 21.47 (2009), pp. 4802–4806.
- [25] Denis Y Kondakov. “Triplet–triplet annihilation in highly efficient fluorescent organic light-emitting diodes: current state and future outlook”. In: *Philosophical Transactions of the Royal Society A: Mathematical, Physical and Engineering Sciences* 373.2044 (2015), p. 20140321.